Journal of Hazardous Materials 192 (2011) 432–439

Contents lists available at ScienceDirect

Journal of Hazardous Materials

journal homepage: www.elsevier.com/locate/jhazmat

Use of pH-sensitive polymer hydrogels in lead removal from aqueous solution

Elizabeth Ramírez[a], S. Guillermina Burillo[b], C. Barrera-Díaz[a,*], Gabriela Roa[a], Bryan Bilyeu[c]

[a] Centro Conjunto de Investigación en Química Sustentable UAEM-UNAM, Carretera Toluca-Atlacomulco, km 14.5, Unidad El Rosedal, C.P. 50200, Toluca, Edo. de México, Méx, México
[b] Instituto de Investigaciones en Ciencias Nucleares UNAM, Mexico
[c] Department of Chemistry, Xavier University of Louisiana, 1 Drexel Drive, New Orleans, Louisiana 70125, USA

ARTICLE INFO

Article history:
Received 26 January 2011
Received in revised form 27 April 2011
Accepted 30 April 2011
Available online 26 May 2011

Keywords:
Gamma ray
Smart hydrogel
Metal removal
Water treatment

ABSTRACT

Three gamma crosslinked polymeric hydrogels were synthesized and evaluated as lead ion sorbents. A crosslinked poly(acrylic acid) hydrogel was compared with two 4-vinylpiridine-grafted poly(acrylic acid) hydrogels (26.74 and 48.1% 4-vinylpiridine). The retention properties for Pb(II) from aqueous solutions of these three polymers were investigated by batch equilibrium procedure. The effects of pH, contact time and Pb(II) concentration were evaluated. The optimal pH range for all polymers was 4–6. The lightly grafted polymer (PAAc-*g*-4VP at 26.74%) exhibited a Pb(II) removal close to 80% at 5 h and above 90% at 24 h. The maximum Pb(II) removal was 117.9 mg g^{-1} of polymer and followed the Freundlich adsorption model. XPS characterization indicates that the carboxyl groups are involved in the Pb(II) removal.

1. Introduction

Lead, is a metal with an ionic radius of 0.132 nm [1] with an oxidation state of (+2) and 0.084 nm for an oxidation state of (+4), with an electronegativity of 1.9 [2] and a density of 11.34 g cm^3 [3] and like many heavy metals, is toxic and carcinogenic and hence presents a threat to human health and the environment when it is discharged into water resources. Because of its toxicity and the tendency for bio-accumulation in the food chain, it is imperative to reduce or eliminate the amount in industrial effluent discharged to the environment [4–6]. Industrial processes like battery manufacturing, metal plating and finishing are prime sources of lead pollution. Lead accumulates mainly in bones, brain, kidney and muscles and may cause serious developmental disorders, impairment, sickness, and death [7].

High levels of lead can be reduced by raising the pH of the solution to form the insoluble lead hydroxide precipitate, but low levels of the free ion persist and require advanced treatment. Additional methods like ion exchange, membrane filtration, and reverse osmosis are effective at further reducing or even eliminating lead but they are expensive [8]. With respect to low concentrations in large volumes of aqueous solution, extraction procedures are uneconomic and precipitation procedures require the addition of relatively large amounts of chemicals, whereas applications of adsorption or ion exchange on solids are advantageous [9]. Adsorption is one of the methods commonly used to remove heavy metal ions from various aqueous solutions with relatively low metal ion concentrations. For this purpose, a lot of materials have been used. Recent examples of this are synthetic polymers [10] and biosorbents like sawdust [11], nut shells [12] and powdered marble [13].

The use of hydrogels (crosslinked hydrophilic polymers or copolymers) as adsorbents for the removal of heavy metals, recovery of dyes, and removal of toxic components from various effluents has been studied [14–17]. Adsorbents with carboxyl, sulphonic, phosphonic and nitrogen groups on their surface favor metal ion adsorption [18–23].

Cross-linked hydrophilic polymers immersed in water can uptake large amount of water depending on the crosslinking density [24]. Due to characteristic properties such as swellability in water, hydrophilicity, biocompatibility and lack of toxicity, hydrogels have been utilized in a wide range of biological, medical, pharmaceutical and environmental applications [25].

Environmental sensitive or "smart" hydrogels are able to change their volume by more than one order of magnitude in response to different parameters such as temperature, pH value, light, ion, and substance concentrations [26]. In this sense, pH responsive polymers are characterized as having ionizable pendant groups that can accept or donate protons, being cationic or anionic respectively [27].

Radiation induced graft copolymerization has received considerable attention for the synthesis of polymeric materials that play important roles today in practical applications of various separation processes due to the fact that this method can be performed without additives [28,29].

* Corresponding author. Tel.: +52 722 2173890; fax: +52 722 2175109.
E-mail addresses: cbd0044@yahoo.com, cbarrera@uaemex.mx (C. Barrera-Díaz).

0304-3894/$ – see front matter © 2011 Elsevier B.V. All rights reserved.
doi:10.1016/j.jhazmat.2011.04.109

In this study, the behavior of lead ions removal from water through a polymer obtained by radiation-induced graft of 4-vinyl pyridine (4VP) onto acrylic acid (AAc) network was evaluated.

2. Materials and methods

2.1. Materials

Acrylic acid (AAc) and 4-vinylpyridine (4-VP) were both obtained from Aldrich (Milwaukee, USA) and purified by distillation in vacuum before use.

2.2. Synthesis of polyacrylic acid network (net-PAAc)

The acrylic acid was polymerized and crosslinked into a polyacrylic acid network gel by gamma radiation. A 1:1 solution of acrylic acid and distilled water was mixed under an argon atmosphere, then gamma irradiated using a GAMMABEAM 651 PT ^{60}Co source with a radiation dose of 10 kGy at a rate of 7.054 kGy/h. The resulting gel was washed in dimethyl formamide (DMF) to remove any residual monomers, then rinsed with methanol and dried in a vacuum oven. After drying, the gel was cut into small cubes of about 2 mm per side and stored in a desiccator until use.

2.3. Graft copolymerization

The 4VP-grafted PAAc hydrogel (*net*-PAAc-g-4VP) was synthesized by gamma radiation. Cubes of the PAAc hydrogel were immersed in a 1:1 mixture of 4VP and distilled water and allowed to swell for 2 h. Under an argon atmosphere, the immersed gels were irradiated with ^{60}Co γ rays for a dose of from 1 to 25 kGy at a rate of 7.05 kGy/h. After irradiation, the samples were washed with DMF for 24 h to remove any residual 4VP. After rinsing with methanol, the samples were dried in a vacuum oven, then stored in a desiccator until use. The degree of grafting was calculated from the percentage increase in the weight of the polyacrylic acid gel after the grafting process as follows:

$$\text{Degree of grafting}\,(\%) = \left[\frac{W_g - W_0}{W_0}\right] \times 100$$

where W_0 and W_g are the weights of the ungrafted and grafted gels, respectively.

Two different grafted copolymers of *net*-PAAc-g-4VP with degrees of grafting of 26.74% and 48.1% were synthesized.

2.4. Thermodynamic study

The existence of Pb(II) complexes in aqueous solution has been reported. Using this information, the distribution diagrams of chemical species were calculated using the MEDUSA program [30–32].

2.5. SEM and EDX

Scanning Electron Microscopy (SEM) and Energy Dispersive X-ray Spectroscopy (EDX) elemental analysis were performed on both the AAc hydrogel and the grafted hydrogels, before and after contact with the aqueous solution, using a JEOL JSM-5900 LV with a DX-4 analyzer. SEM provides secondary electron images of the surface with resolution in the micrometer range, while EDX offers in situ chemical analysis of the bulk.

2.6. Fourier Transform Infrared Spectroscopy (FTIR)

Net-AAc and *net*-PAAc-*g*-4VP were analyzed with a Nicolet Magna-IR 550 to observe the changes in the chemical bonds and structure and to ensure that graft polymerization had taken place.

2.7. Thermogravimetric analysis (TGA)

The hydrogels were analyzed for thermal stability and thermal decomposition kinetics with a TGA Q50 (TA Instruments, New Castle, DE) to evaluate structural differences and changes.

2.8. Differential Scanning Calorimetry (DSC)

DSC studies were performed on a TA Instruments Model 2010 to compare the glass transition temperatures of the networked and grafted hydrogels to evaluate the differences in crosslinking and chemical structure.

2.9. X-ray photoelectron spectroscopy (XPS)

The XPS wide and narrow spectra were acquired using a JEOL JPS-9200, equipped with a Mg X-ray source (1253.6 eV) at 200 W, analyzing a 1 mm^2 area under a 1×10^{-6} Pa vacuum. The spectra were analyzed using the Specsurf^{TM} software included with the instrument and all spectra were charge corrected by means of the adventitious carbon signal (C 1s) at 284.5 eV. The Shirley method was used for background subtraction and the Gauss–Lorentz method was used for the curve fitting.

XPS analysis of the *net*-PAAc-*g*-4VP before and after the lead adsorption was carried out to determine the atoms present on the polymer surface and to elucidate possible lead interactions with the polymer.

2.10. Adsorption of Pb(II) by polymer

In order to evaluate the Pb(II) removal capacity of the polymers, batch equilibrium tests were conducted. The *net*-PAAc and *net*-PAAc-*g*-4VP samples (dry cubes) were put in contact with the aqueous Pb(II) solutions at room temperature. All solutions were prepared with analytical grade reagents, using lead nitrate (Merck, 99.5%) and deionized water. The mixtures were stirred at 8 rpm, and then the phases were separated by filtration and the Pb(II) in solution was evaluated. Contact times varied from 0.5 to 24 h. Also, the effect of the pH on lead sorption was determined by using different pH values from 2 to 6, monitored with a Radiometer Analytical Meterlab® Ion 450 pH meter. The initial lead concentration in all cases was 10 mg L^{-1}. For isotherm experiments, lead concentration varied from 4 to 16 mg L^{-1} and contact time in all cases was 24 h. Duplicate experiments permitted averaging of the results.

The lead removal was calculated as follows:

$$\%\,\text{removal} = 100 - \frac{\text{Cf} \times 100}{\text{Co}}$$

where Cf, final lead concentration; Co, initial lead concentration.

For the isotherms:

$$\text{Qe} = \frac{V(\text{Co} - \text{Ce})}{w}$$

where Qe, sorption capacity; V, volume; Co, initial lead concentration; Ce, equilibrium lead concentration; w, polymer weight.

2.11. Quantification of Pb(II) concentration in solution

The concentration of Pb(II) ions in solution, before and after the sorption process, was determined using a Perkin-Elmer 2380

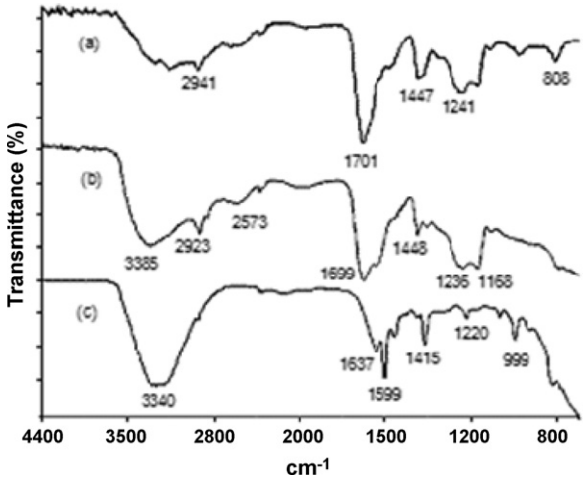

Fig. 1. (a) *Net*-PAAc, (b) *net*-PAAc-*g*-4VP (26.74%) and (c) 4VP Fourier transformation infrared spectra.

atomic absorption spectrophotometer. All calibrations and procedures were carried out in accordance with AWWA standards. The effect of the pH on lead sorption was measured by changing the pH of the aqueous solution in a range of 2–6 units.

3. Results and discussion

3.1. FTIR analysis

The *net*-PAAc and *net*-PAAc-g-4VP (26.74%) infrared spectra are shown in Fig. 1. Fig. 1a shows that the *net*-PAAc FTIR displayed a band at 1701 cm^{-1} indicating the stretching of a carbonyl group, moreover methylene groups signals are observed at 2941 and 1447 cm^{-1}. On the other hand, the carbonyl group stretching in Fig. 1b is at 1699 cm^{-1}, the methylene groups stretching is at 2923 cm^{-1} and a characteristic secondary amine band is present at 3385 cm^{-1}, indicating that graft polymerization takes place.

The broad band ranging from about 3100 to 3700 cm^{-1} corresponds usually to the combination of the stretching vibration bands of both OH and NH groups [10]; shifted slightly after the sorption, indicating that stretching vibrations were affected by the bound lead (Fig. 2). Other changes due to the same reason were observed like the peak at 2912 cm^{-1} before the lead adsorption and 2908 cm^{-1} afterwards. This band region may be assigned to both C–H and O–H stretching. These shifts suggest that the hydroxyl groups are involved in lead adsorption and the carbonyls

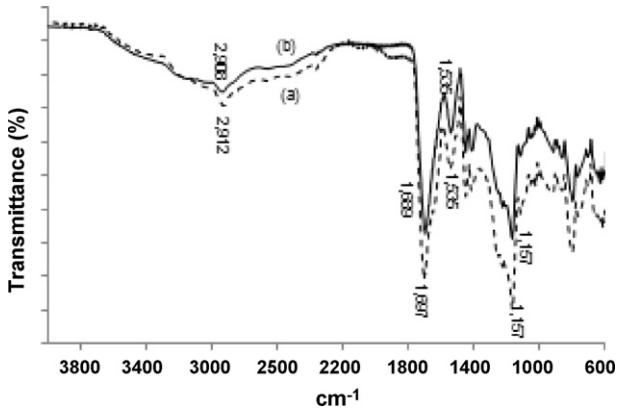

Fig. 2. FTIR spectra of *net*-PAAc-*g*-4VP (26.74%) (a) before lead adsorption and (b) *net*-PAAc-*g*-4VP (26.74%) after lead adsorption.

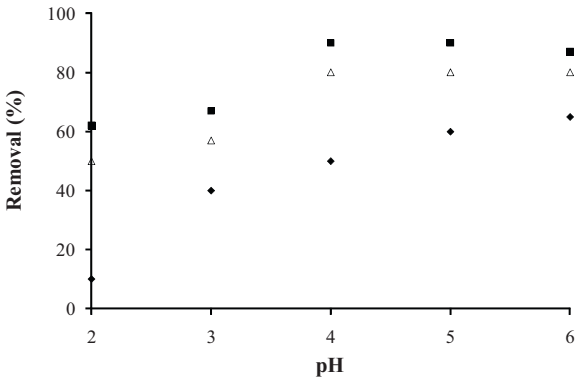

Fig. 3. Effect of the pH on the Pb(II) removal at 24 h of contact time with a Pb(II) initial concentration of 10 mg L^{-1}. (■) *Net*-PAAc-*g*-4VP (26.74%), (△) *net*-PAAc-*g*-4VP (48.1%) and (♦) *net*-PAAc.

are affected by it. On the other hand, the peak at 1157 cm^{-1} corresponding to OH bending [33] did not change. With this information we conclude that both O–H and N–H functional groups contained in the polymer structure are involved in the lead ions adsorption process.

3.2. pH effect on lead sorption

The effect of solution pH on the adsorption of lead ions is shown in Fig. 3. *Net*-PAAc and both grafted polymers display a general trend of increasing Pb(II) removal with increasing solution pH until peaking at pH 4 and decreasing slightly at higher values. The pH effect in *net*-PAAc was drastic with Pb(II) removal close to 90% at pH 4 in contrast to 6% at pH 2. This is likely due to increased competition of protons with metal ions at the active sites on the carboxylates in more acidic conditions [34]. The effect was less dramatic in the grafted polymers, possibly due to the effect of the unshared pyridine electron pairs being located in sp^2 orbitals instead of sp^3. Thus, these electron pairs are more bound to the nucleus and the protons do not attack so easily [35]. In general, this behavior has been observed previously in aminated polyacylonitrile fibers where at acidic pH values (below 2.3) the strong electrical repulsion prevented the lead ions from interacting with the surface of the polymer, resulting in poor adsorption. With the increase of solution pH values, the electrical repulsion force became weaker and the lead ions may be transported to the surface of the polymer and become attached on the surface [10].

3.3. Predominant chemical species in aqueous solution

The lead species diagram is presented in Fig. 4. As expected, the predominant form for lead from pH values 0–6 is Pb(II). Taking into account this information and the previous experimental data in which maximum lead removal takes place in a pH value of 4, we precede the experimental performance using this pH value.

3.4. Sorption results

Fig. 5 shows the experimental plot obtained for Pb(II) removal from aqueous solution as a function of contact time with the polymer. Note that the less grafted polymer (*net*-PAAc-*g*-4VP 26.74%) had the highest Pb(II) removal rate. In 5 h it achieved a Pb(II) reduction around 80% compared with *net*-PAAc at about 60%. This confirms that the introduction of 4-vinyl pyridine on *net*-PAAc enhanced the adsorption of lead ions. It has been reported that an amino group on an adsorbent is one of the most effective chelating groups for adsorption of heavy metal ions from aqueous solutions

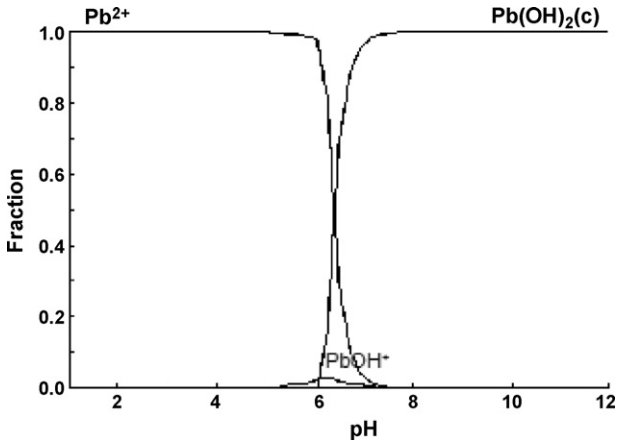

Fig. 4. Simulation of lead species in aqueous solution at different pH values with a concentration of 10 mg L^{-1} in a Medusa program.

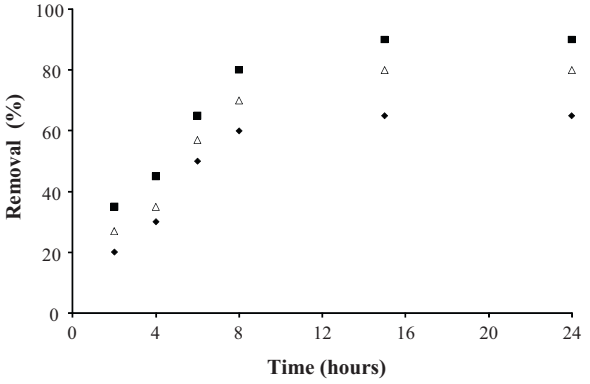

Fig. 5. Experimental Pb(II) removal from aqueous solution as a function of contact time, with Pb(II) initial concentration of 10 mg L^{-1}. (■) *Net*-PAAc-*g*-4VP (26.74%), (△) *net*-PAAc-*g*-4VP (48.1%) and (♦) *net*-PAAc.

[10]. It is also observed that adsorption lead ions increased rapidly in the first 8 h and then augmented slowly. This type of adsorption behavior is typical of the specific adsorption process in which adsorption rate is dependent upon the number of available adsorption sites on the surface of the adsorbent [36].

We also adjusted experimental data to the mathematical models of Elovich, pseudo-first and second-order. Table 1 shows the degree of correlation of the data with the models. As indicated by Table 1 pseudo-second-order type has the highest correlation which agrees with the previous discussion.

3.5. Adsorption isotherms

Lead adsorption isotherms were fitted to Langmuir and Freundlich equations in order to determine the mechanism (homogeneous or heterogeneous adsorption) and to calculate the maximum polymer adsorption capacity of the *net*-PAAc-*g*-4VP, 26.74%. The Pb(II) initial concentration was varied from 4 to 16 mg L^{-1} with 24 h of contact time to obtain the experimental

Table 1
Correlation factors for experimental results fitted to models.

PAAc-g-4VP 26.74%	
Model	R^2
Elovich	0.941
Pseudo-first order	0.946
Pseudo-second order	0.972

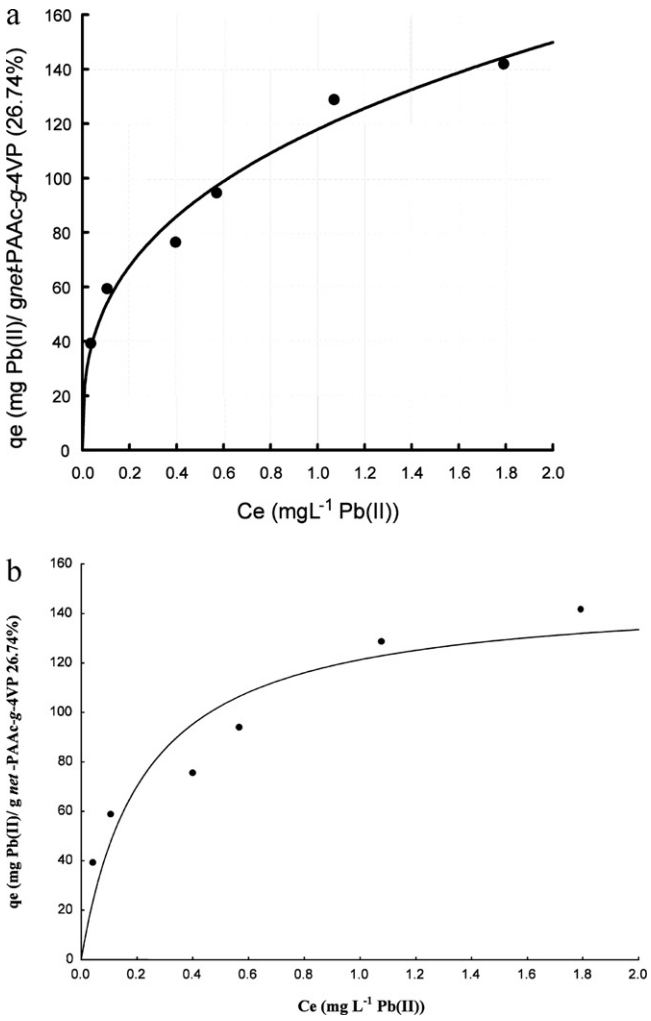

Fig. 6. (a) Experimental data fitted to Freundlich isotherm model. (b) Experimental data fitted to Langmuir isotherm model.

adsorption data. As shown in Fig. 6a, the Freundlich model describes experimental data with a correlation factor of 0.97, whereas the Langmuir model (Fig. 6b) is only 0.86. The Freundlich model assumes heterogeneous adsorption sites, whereas the Langmuir model assumes all sites are similar. From the experimental results in Fig. 6a, the maximum removal was 117.9 mg of lead ions per gram of *net*-PAAc-*g*-4VP with 26.74% grafting.

3.6. Comparison with other sorbents

Although a direct comparison of *net*-PAAc-g-4VP (26.74%) with other sorbents is not feasible due to different experimental conditions applied, the *net*-PAAc-g-4VP (26.74%) adsorption capacity of 117.9 mg of Pb(II)/g is comparatively higher than other sorbents (Table 2).

3.7. SEM analysis

Images of *net*-PAAc and the grafted polymer recorded at 1000× are shown in Fig. 7a and b. The morphology of the *net*-PAAc (Fig. 7a) is not a homogeneous architecture and the pore size is larger than the grafted polymer probably due to the high hydrophilicity of the gel. On the other hand, the effect of the 4VP on the *net*-PAAc-*g*-4VP (26.74%) (Fig. 7b) results in a more homogeneous network structure because the system is now less hydrophilic.

Table 2
Comparison of Pb(II) sorption capacity of different sorbent materials.

Adsorbent	Reported sorption capacities (mg g^{-1})	Ref.
Chitosan	16.36	[37]
Chabazite	6.00	[38]
Kaolinite	1.41	[39]
Illite	4.29	[39]
Bentonite	20	[40]
Blast-furnace slag	40	[41]
Sugar beet pulp (p-DW)	50	[42]
Zn(II)PMA	20.11	[43]
Cu(II)PMA	6.22	[44]
APANAF	76	[10]
Net-PAAc-*g*-4VP	117.91	Present work

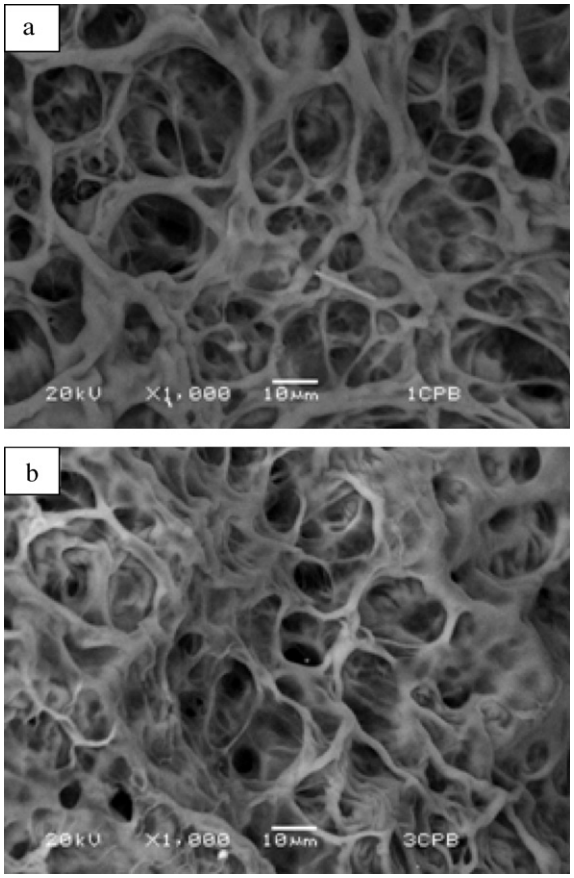

Fig. 7. Secondary electron image of (a) *net*-PAAc and (b) *net*-PAAc-*g*-4VP (26.74%). The magnification marker is 10 μm.

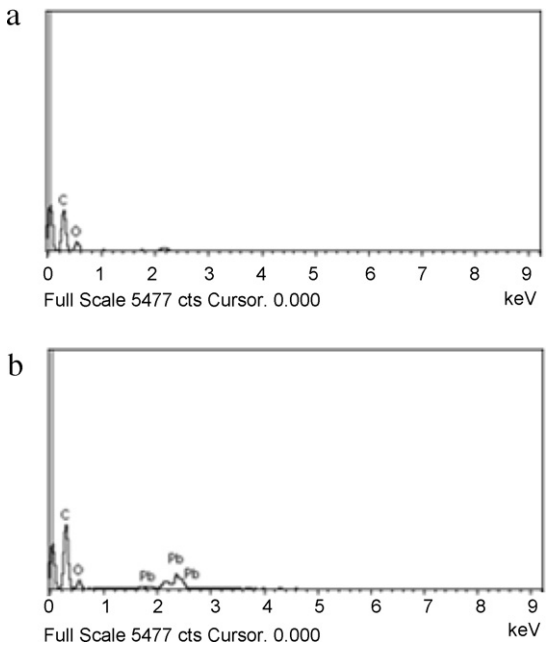

Fig. 8. Elemental analysis of the *net*-PAAc-*g*-4VP (26.74%) surface before (a) and after (b) contact with Pb(II) aqueous solution.

3.8. EDX

EDX elemental analysis was done before and after contact with the lead aqueous solution. While the EDX of the unexposed *net*-PAAc-g-4VP (26.74%) hydrogel (Fig. 8a) only indicates the carbon and oxygen of the polymer components, lead is also detected on the surface (Fig. 8b) after the sorption process, indicating that lead was adsorbed onto the surface.

3.9. Differential Scanning Calorimetry (DSC)

The glass transition temperatures (T_g) of *net*-PAAc (a) and *net*-PAAc-*g*-4VP (26.74%) (b) are shown in Fig. 9. Note that the T_g is higher for the grafted polymer than the *net*-PAAc probably due to higher crosslink density and possibly greater noncovalent interactions.

3.10. Thermogravimetric analysis

The beginning of thermal degradation, indicated by the 10% weight loss, is lower for the *net*-PAAC-*g*-4VP (26.74%) (Fig. 10b) than for the ungrafted *net*-PAAC (Fig. 10a), which indicates that the grafted 4VP is likely decomposing before the main network which

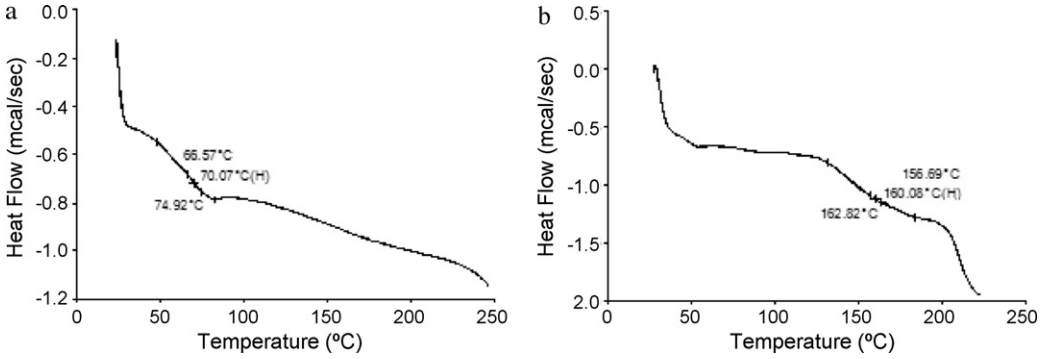

Fig. 9. Differential Scanning Calorimetry of (a) *net*-PAAc and (b) *net*-PAAc-*g*-4VP (26.74%).

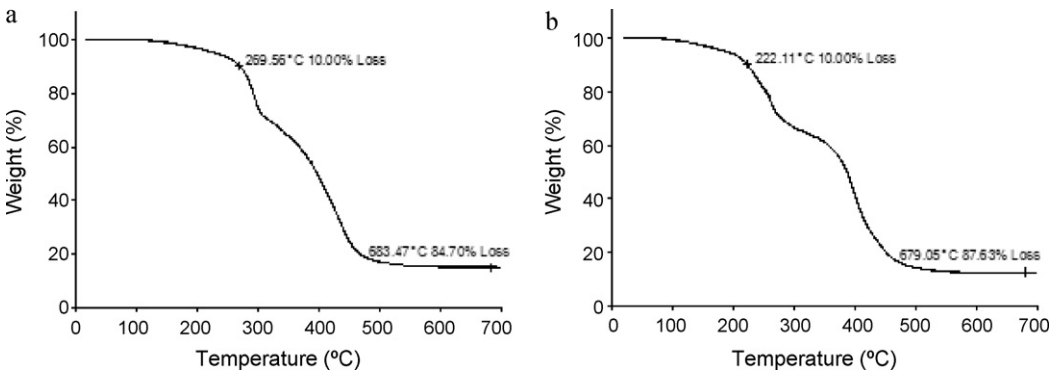

Fig. 10. Thermogravimetric analysis of (a) *net*-PAAc and (b) *net*-PAAc-*g*-4VP (26.74%).

suggests that the 4VP unit is bonded to the network polymer rather than being incorporated into the polymer chain itself. After the 4VP portion fully decomposes, then there is a step change in the process, where it matches the appearance and slope of the ungrafted network. Final thermal decomposition ends at about the same temperature for both networks. The slightly greater weight loss for the grafted network as opposed to the ungrafted one is likely due to that grafted component completely volatilizing.

3.11. X-ray photoelectron spectroscopy

Electrons of the sample are excited and the kinetic energy of ejected photoelectrons is measured in XPS analysis. This energy depends on the electrons bond energy, and the results indicate the presence of species on the surface of adsorbents. In this way, interactions between a metal ion and an atom on the surface of the adsorbent can be identified. The XPS wide spectra of

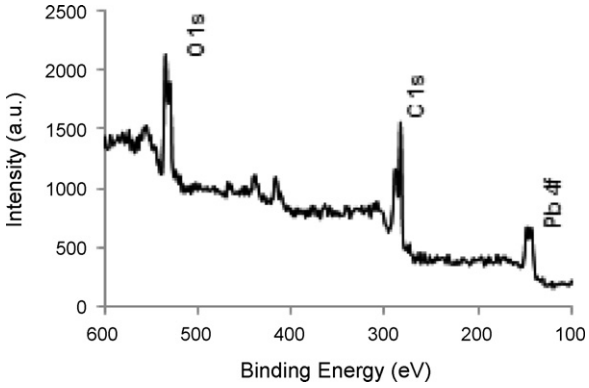

Fig. 11. *Net*-PAAc-*g*-4VP (26.74%) XPS spectra after lead ions adsorption.

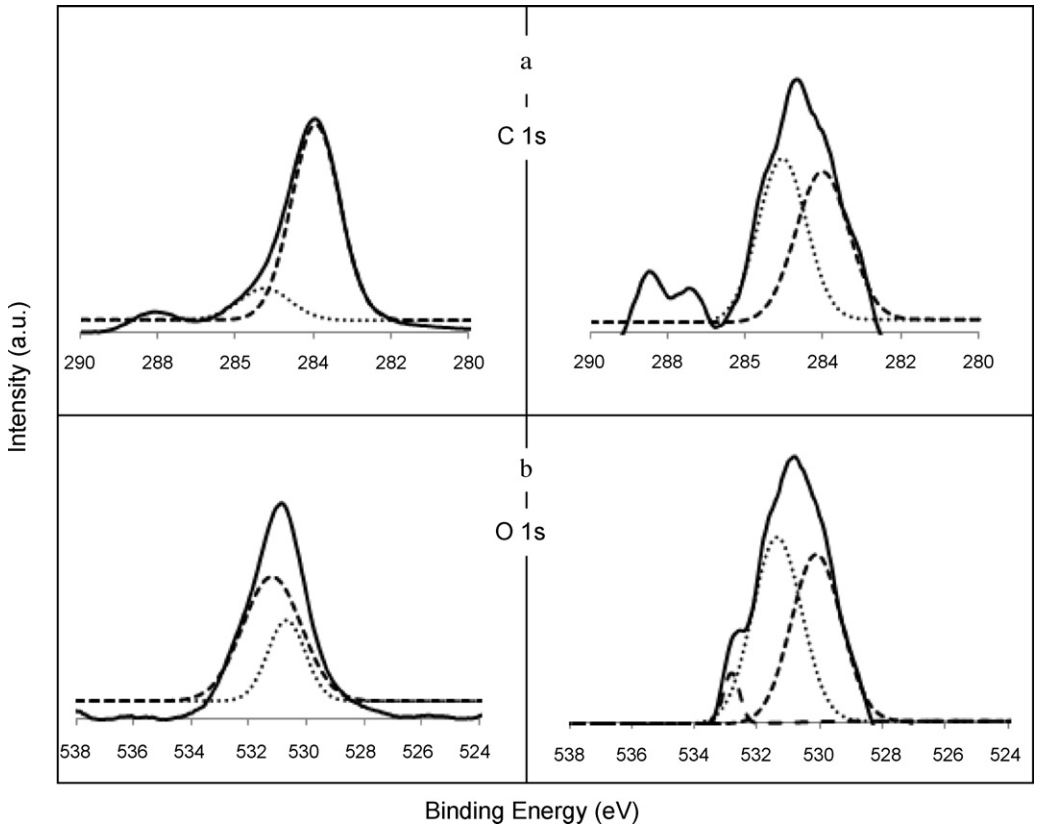

Fig. 12. XPS curve fitting spectra of the C 1s and O 1s signals for *net*-PAAc-*g*-4VP (26.74%) (a) before and (b) after lead contact (— component 1, *** component 2 and -- component 3).

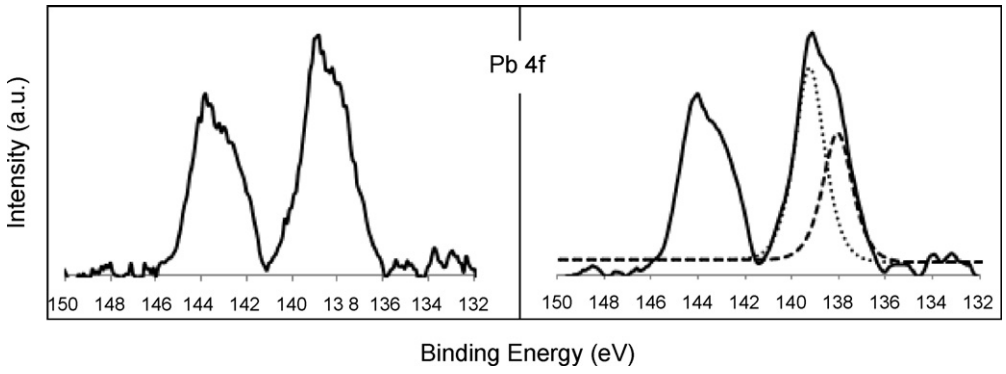

Fig. 13. XPS curve fitting spectra of the Pb 4f signals for *net*-PAAc-*g*-4VP (26.74%) after lead contact (— component 1, *** component 2).

net-PAAc-*g*-4VP (26.74%) after lead contact are shown in Fig. 11. The lead signals present in grafted polymer spectra suggest that it is interacting with the adsorbent.

Fig. 12a and b shows the curve fitting analysis of the C 1s and O 1s signals respectively, before and after lead contact. It can be seen from the C 1s spectra that 3 signals were present before contact with lead ions, the signal labeled as component 1 is due to the C–C signal (≈284 eV), component 2 corresponds to the C–O group (285.3 eV), the signal at about 288 eV is the C=O signal [45]. After contact with lead ions the shape of the signals change, likely because of an interaction between lead ions and the oxygens bonded to the carbons. This is confirmed with the analysis of the oxygen signal; before contact 2 peaks fit the signal, one of them corresponds to C–OH, and the other one to C=O groups. After the lead contact the peaks shift and a new signal for the oxygen and lead interaction appears at 532.857 eV.

Finally, in Fig. 13 the lead photoelectrons are shown. The 2 signals appearing at 137.8 and 139 eV confirm the interaction of the lead ions with the oxygens present in net-PAAc-*g*-4VP and match the analysis of the C 1s and O 1s signals discussed above

4. Conclusions

The net-PAAc hydrogel is an effective lead sorbent, but is significantly improved by grafting 4VP onto the crosslinked network and is most effective in the pH range 4–6. The 26.74% grafted PAAc-*g*-4VP was slightly more effective than the heavier grafted 48.1% and significantly more effective than the ungrafted *net*-PAAc. The heterogeneous sites implied by the fit to the Freundlich model were identified as C–OH and C=O from the XPS results. The maximum capacity of the 26.74% grafted PAAc-*g*-4VP was 117.9 mg of Pb(II) per gram of polymer.

Acknowledgments

The authors thank F. García and B. Leal from ICN UNAM for technical assistance. This work was supported by DGAPA UNAM Grant IN200306 (México).

References

[1] A. Vértes, S. Nagy, Z. Klencsár, Handbook of Nuclear Chemistry, Springer, Kluwer Academic Publishers, Dordrecht, The Netherlands, 2003.
[2] P. Manning, Chemical Bonds, Infobase Publishing, New York, 2009.
[3] J.C. Kotz, P. Treichel, G.C. Weaver, Chemistry and Chemical Reactivity, Cengage Learning, Thomson, Canada, 2006.
[4] S.V. Dimitrova, Use of granular slag columns for lead removal, Water Res. 36 (2002) 4001–4008.
[5] V.J. Inglezakis, M.D. Loizidou, H.P. Grigoropoulou, Equilibrium and kinetic ion exchange studies of Pb^{2+}, Cr^{3+}, Fe^{3+} and Cu^{2+} on natural clinoptilolite, Water Res. 36 (2002) 2784–2792.
[6] A. Özverdi, M. Erdem, Cu^{2+}, Cd^{2+} and Pb^{2+} adsorption from aqueous solutions by pyrite and synthetic iron sulphide, J. Hazard. Mater. 137 (2006) 626–632.
[7] A. Groffman, S. Peterson, D. Brookins, Removing lead from wastewater using zeolites, Water Environ. Technol. 5 (1992) 54–59.
[8] L. Bernabé, Rivas, B. Quilodrán, E. Quiroz, Trace metal ion retention properties of crosslinked poly(4-vinylpyridine) and poly(acrylic acid), J. Appl. Polym. Sci. 92 (2004) 2908–2916.
[9] B.S. Kim, S.T. Lim, Removal of heavy metal ions from water by cross-linked carboxymethyl corn starch, Carbohydr. Polym. 39 (1999) 217–223.
[10] S. Deng, R. Bai, J.P. Chen, Aminated polyacrylonitrile fibers for lead and copper removal, Langmuir 19 (2003) 5058–5064.
[11] F. Kaczala, M. Marques, W. Hogland, lead and vanadium removal from a real industrial wastewater by gravitational settling/sedimentation and sorption onto Pinus sylvestris sawdust, Bioresour. Technol. 100 (2009) 235–243.
[12] E. Pehlivan, T. Altun, S. Cetin, M.I. Bhanger, Shells of hazelnut (Corylus avellana) and almond (Prunus dulcis) lead sorption by waste biomass of hazelnut and almond shell, J. Hazard. Mater. 167 (2009) 1203–1208.
[13] S.E. Ghazy, A.H.M. Gad, Lead separation by sorption onto powdered marble waste, Arab. J. Chem., Available online 9 November 2010, in press. doi:10.1016/j.arabjc.2010.10.031.
[14] W. Li, H. Zhao, P.R. Teasdale, R. John, S. Zhang, Synthesis and characterisation of a polyacrylamide–polyacrylic acid copolymer hydrogel for environmental analysis of Cu and Cd, React. Funct. Polym. 52 (2002) 31–41.
[15] G.N. Manju, K. Anoop-Krishnan, V.B. Vinod, T.S. Anirudhan, An investigation into the sorption of heavy metals from wastewaters by polyacrylamide-grafted iron(III) oxide, J. Hazard. Mater. 91 (2002) 221–238.
[16] S. Ekici, Y. Isikver, N. Sahiner, D. Saraydin, Adsorption of some textile dyes onto crosslinked poly(N-vinylpyrrolidone), Adsorpt. Sci. Technol. 21 (2003) 651–659.
[17] S. Wang, Y. Boyjoo, A. Choueib, Z.H. Zhu, Removal of dyes from aqueous solution using fly ash and red mud, Water Res. 39 (2005) 129–138.
[18] J.P. Chen, L.A. Hong, S.N. Wu, L. Wang, Elucidation of interactions between metal ions and Ca alginate-based ion-exchange resin by spectroscopic analysis and modeling simulation, Langmuir 18 (2002) 9413–9421.
[19] L. Jin, R.B. Bai, Mechanisms of lead adsorption on chitosan/PVA hydrogel beads, Langmuir 18 (2002) 9765–9770.
[20] R. Coskun, M. Yigitoglu, N.J. Sacak, Adsorption behavior of copper(II) ion from aqueous solution on methacrylic acid-grafted poly(ethylene terephthalate) fibers, J. Appl. Polym. Sci. 75 (2000) 766–772.
[21] S. Lancour, J.C. Bollinger, B. Serpaud, P. Chantron, R. Arcos, Removal of heavy metals in industrial wastewaters by ion-exchanger grafted textiles, Anal. Chim. Acta 428 (2001) 121–132.
[22] C.A. Borgo, Y.J. Gushikem, Zirconium phosphate dispersed on a cellulose fiber surface: preparation, characterization, and selective adsorption of Li^+, Na^+, and K^+ from aqueous solution, J. Colloid Interface Sci. 246 (2002) 343–347.
[23] R. Liu, Y. Li, H. Tang, Synthesis and characteristics of chelating fibers containing imidazoline group or thioamide group, J. Appl. Polym. Sci. 83 (2002) 1608–1616.
[24] K.F. Arndt, M. Knörgen, S. Richter, T. Schmidt, Modern magnetic resonance, in: A.W. Graham (Ed.), Part 1: Applications in Chemistry, Biological and Marine Sciences, 1st ed., Springer, The Netherlands, 2008, pp. 187–193.
[25] B. Jankovic, B. Adnadevic, J. Jovanovic, Isothermal kinetics of dehydration of equilibrium swollen poly(acrylic acid) hydrogel, J. Therm. Anal. Calorim. 92 (2008) 821–827.
[26] A.E. English, E.R. Edelman, T. Tanaka, Polymer hydrogel phase transitions, in: T. Tanaka (Ed.), Experimental Methods in Polymer Science: Modern Methods in Polymer Research and Technology, Academic Press, New York, 2000, pp. 547–550.
[27] D. Velasco, C. Elvira, J. San Ramon, New stimuli-responsive polymers derived from morpholine and pyrrolidine, J. Mater. Sci.: Mater. Med. 19 (2008) 1453–1458.
[28] H. Kamal, E-S.A. Hegazy, A.E-K.B. Mostafa, A.A. Maksoud, Radiation-modified copolymer for the extraction of metal ions from water, J. Appl. Polym. Sci. 106 (2007) 3366–3374.
[29] A. Licea, R. Salgado, E. Lugo, K. Friedrich, Incorporation of acid polymethacrylates into temperature sensitive hydrogels using electron beam irradiation, Polym. Bull. 60 (2008) 701–712.

[30] C. Baes, R. Mesmer, The Hydrolysis of Cations, Robert E. Kriegeer, Malabar, Florida, 1986.
[31] M.R. Smith, A.E. Martell, Critical Stability Constants, Plenum Press, New York, 1974.
[32] I. Puigdomenech, Hydrochemical Equilibrium Constants Database (MEDUSA), Royal Institute of Technology, Stockholm, 1997.
[33] L. Jin, R. Bai, Mechanisms of lead adsorption on chitosan/PVA hydrogel beads, Langmuir 18 (2002) 9765–9770.
[34] B. Rivas, Polímeros funcionales con capacidad para retener Iones metálicos con impacto en el medio ambiente, Ciencia Ahora 20 (2007) 70–79.
[35] C.B. Fryhle, T.W.G. Solomons, Organic Chemistry, seventh ed., John Wiley & Sons Inc., New York, 1999.
[36] Y.S. Ho, G. McKay, Pseudo-second order model for sorption processes, Process Biochem. 34 (1999) 451–465.
[37] C.Y. Huang, Ch. Chung, M.R. Liou, Adsorption of Cu(II) and Ni(II) by pelletized biopolymer, J. Hazard. Mater. 45 (1996) 265–277.
[38] S.K. Ouki, M. Kavanagh, Performance of natural zeolites for the treatment of mixed metal-contaminated effluents, Waste Manage. Res. 15 (1997) 383–394.
[39] V. Chantawong, N.W. Harvey, V.N. Bashkin, Comparison of heavy metal adsorptions by Thai kaolin and ballclay, Water Air Soil Pollut. 148 (2003) 111–125.
[40] R. Naseem, S.S. Tahir, Removal of Pb(II) from aqueous/acidic solutions by using bentonite as an adsorbent, Water Res. 35 (2001) 3982–3986.
[41] S.K. Srivastava, V.K. Gupta, D. Mohan, Removal of lead and chromium by activated slag – a blast-furnace waste, J. Environ. Eng. 123 (1997) 461–468.
[42] C. Gérente, P. Couespel du Mesnil, Y. Andrès, J.F. Thibault, P. Le Cloirec, Removal of metal ions from aqueous solution on low cost natural polysaccharides, sorption mechanism approach, React. Funct. Polym. 46 (2000) 135–144.
[43] F. Ureña, C. Barrera, B. Bilyeu, Gamma radiation-polymerized Zn(II) methacrylate as a sorbent for removal of Pb(II) Ions from wastewater, Ind. Eng. Chem. Res. 46 (2007) 3382–3389.
[44] C. Barrera, M. Palomar, M. Romero, F. Ureña, Lead removal from wastewater using Cu(II) polymethacrylate formed by gamma radiation, J. Polym. Res. 12 (2005) 421–428.
[45] Y.Q. Zhu, E.T. Kang, K.G. Neoh, T. Osipowicz, L. Chan, Plasma graft copolymerization of 4-vinylpyridine on dense and porous SiLK for electroless plating of copper and for retardation of copper diffusion, J. Electrochem. Soc. 152 (2005) F107–F114.